

Thermal Property and Hydrogen Bonding in Blends of Poly(vinylphenol) and Poly(hydroxyether of Bisphenol A)

Shiao-Wei Kuo, Chen-Lung Lin, Hew-Der Wu and Feng-Chih Chang*

Institute of Applied Chemistry, National Chiao Tung University, Hsinchu, Taiwan, ROC

(*Author for correspondence; Tel: 886-3-5727077; Fax: 886-3-5723764; E-mail: changfc@cc.nctu.edu.tw)

Received 16 April 2002; accepted in revised form 29 January 2003

Key words: phenoxy, polymer blend, poly(vinylphenol)

Abstract

The thermal property and hydrogen bonding in polymer blends of poly(vinylphenol) (PVPh) and poly(hydroxyether of bisphenol A) (phenoxy) were investigated by differential scanning calorimetry (DSC), Fourier transform infrared spectroscopy (FTIR) and solid-state nuclear magnetic resonance (NMR). This PVPh/phenoxy blend shows single composition-dependent glass transition temperature over the entire compositions, indicating that the hydrogen bonding exists between the hydroxyl of PVPh and hydroxyl of phenoxy. The negative T_g deviation of the PVPh/phenoxy blend indicates the strong intermolecular hydrogen-bonding interaction. The inter-association constant for the PVPh/phenoxy blend is significantly higher than self-association constants of PVPh and phenoxy, revealing that the tendency toward hydrogen bonding between PVPh and phenoxy is more favorable than the intra-hydrogen bonding of the PVPh and phenoxy in the blend.

Introduction

The miscibility and hydrogen bonding behavior of the poly(vinylphenol) (PVPh) and a number of polymers containing functional groups such as carbonyl, ether and pyridine have been widely reported to be miscible in the amorphous phase due to the presence of intermolecular hydrogen bonding between the PVPh hydroxyl and the functional group of the second polymer [1–13]. However, for our knowledge, no research has been reported concerning the blend between PVPh and polymer containing hydroxyls. The phenoxy is a well-known polymer to possess main chain hydroxyls hydrogen-bonding donor. Polymer blends of phenoxy with polyoxides, polyester and polymethacrylate have been widely studied lately [14–20].

Based on structures of PVPh and phenoxy, strong self-association hydrogen bonding is expected from these two homopolymers. In the PVPh/phenoxy blend, the magnitude of inter-association relative to their self-associations dictates the contribution of the free energy of mixing and its miscibility. For example, if the inter-association of PVPh/phenoxy blend is more favorable than self-associations of both PVPh and phenoxy, the polymer blend is expected to be miscible. Conversely, if self-association are more favorable than the inter-association, the resulted blend tends to be immiscible or partially miscible. In general, these self- and inter-association equilibrium constants can be calculated using Fourier transform infrared spectroscopy based on the Painter–Coleman association model (PCAM) [21].

The purpose of the present work is to study the miscibility and hydrogen bonding behavior of PVPh/phenoxy

blends. The effect of hydrogen bonding on the miscibility of the PVPh/phenoxy blend will be investigated using differential scanning calorimetry (DSC), Fourier transform infrared spectroscopy and solid state NMR.

Experimental

Materials

The poly(vinyl phenol) (PVPh) with a $M_w = 9000$ – 10000 was purchased from Polyscience Inc. of USA. The phenoxy was obtained from the Union Carbide Co., with $M_n = 23000$ and $M_w = 48000$. The chemical structures of PVPh and phenoxy are illustrated in Figure 1. The phenoxy analog, 2-propanol and the PVPh analog, 4-ethylphenol were purchased from the Aldrich Chemical Company.

Blend Preparations

Blends of PVPh/phenoxy with different compositions were prepared by solution blend. THF solution containing 5 wt% polymer mixture was stirred for 6–8 h, and the solution was allowed to evaporate slowly at 50 °C for 1 day. The film of the blend was then dried at 80 °C for 2 days to ensure total elimination of the solvent.

Differential Scanning Calorimetry

The glass transition temperature of the blend was determined by using a DSC from Du-Pont (DSC-9000) with a scan rate of 20 °C/min and the temperature range of 30–150 °C. The measurement was made using a 5–10 mg sample on a DSC

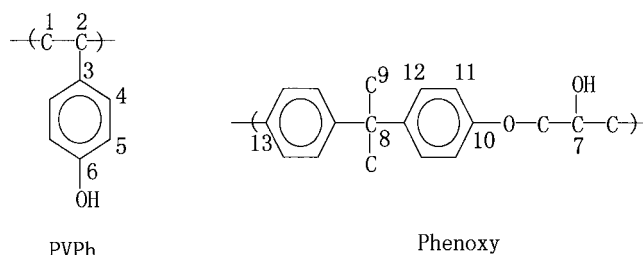


Figure 1. Chemical structures of PVPh and phenoxy and their atom numbering schemes.

sample cell after the sample was quickly cooled to -20°C from the melt of the first scan. The glass transition temperature was obtained as the inflection point of the jump heat capacity with scan rate of $20^{\circ}\text{C}/\text{min}$ and temperature range of -20 to 200°C .

Infrared Spectroscopy

Infrared spectra were recorded on a Nicolet Avatar 320 FT-IR spectrophotometer and 32 scans were collected with a spectral resolution 1 cm^{-1} . Infrared spectra of polymer blend films were determined by using the conventional NaCl disk method. The THF solution containing the blend was cast onto NaCl disk and dried under condition similar to that used in the bulk preparation. The film used in this study was sufficiently thin to obey the Beer–Lambert law. IR spectra recorded at elevated temperatures were obtained by using a cell mounted inside the temperature-controlled compartment of the spectrometer. For the solution sample, an adequately sealed cell with NaCl windows and 0.2 mm sample thickness was used. A single optical path was used to study the inter-association equilibrium constant between model compounds of 4-ethylphenol and 2-propanol. All model compound solutions in the absorption range obey the Beer–Lambert law. Cyclohexane was selected as the solvent because the specific conformation of the cyclohexane is favorable in this study.

Solid State NMR

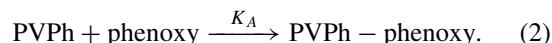
High resolution solid state NMR experiments were carried out on a Bruker DSX-400 Spectrometer operating at resonance frequencies of 399.53 and 100.47 MHz for ^1H and ^{13}C , respectively. The ^{13}C CP/MAS spectra were measured with a $3.9\ \mu\text{s}$ 90° pulse, 3 s pulse delay time, acquisition time of 30 ms and 2048 scans. All NMR spectra were taken at 300 K using broad band proton decoupling and a normal cross-polarization pulse sequence. A magic angle sample spinning (MAS) rate of 5.4 kHz was used to avoid absorption overlapping.

Results and Discussion

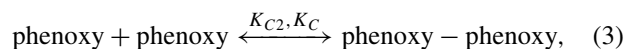
Estimation of K_A Value between PVPh and Phenoxy

The usual interaction scheme based on competing equilibrium according to the Painter–Coleman association model is

described as follows:



The inter-association equilibrium constant K_A reflects the tendency of the hydrogen bonding between PVPh and phenoxy. However, the phenoxy is also considered to possess strong self-association hydrogen bonding as follows:



where K_2 , K_B and K_{C2} , K_C are self-association equilibrium constants of PVPh and phenoxy, respectively. Here, the K_2 and K_B is almost the same as K_{C2} and K_C , which depends on the considering self-association polymer and we defined the self-association constants of the PVPh ($K_2 = 21.0$ and $K_B = 66.8$) and phenoxy ($K_{C2} = 14.4$ and $K_C = 25.6$) that have been determined previously by Coleman et al. and Espi et al. [21, 22]. All these association parameters are important in determining the competition between the self- and the inter-hydrogen bonding within the PVPh/phenoxy blend. In this study, the K_A value between PVPh and phenoxy was determined by using model compounds of 4-ethylphenol and 2-propanol based on the classical Coggesthall and Saier methodology [23]. Cyclohexane is considered as an inert diluent which does not exist any fundamental vibration frequency in the hydroxyl stretching regions of the infrared spectrum. However, the solution containing large quantities of cyclohexane inevitably shows overtone and combination bands which will interfere in the analytic range of interest. In order to eliminate these overtone and combination contributions from the spectra of the Eph/cyclohexane and Eph/propanol/cyclohexane, the spectrum of the pure cyclohexane was digitally subtracted as shown in Figure 2. On subtraction of the pure cyclohexane spectrum, the relatively sharp free hydroxyl stretching is the only obvious present. Figure 3 shows free hydroxyl absorption of 0.02 M-ethylphenol and various concentrations of 2-propanol. The intensity of the free hydroxyl band absorption at 3620 cm^{-1}

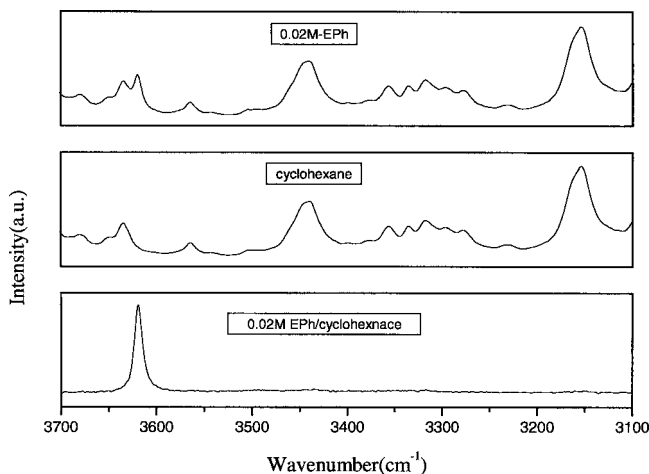


Figure 2. Infrared spectra recorded at room temperature in the region from 3100 – 3700 cm^{-1} .

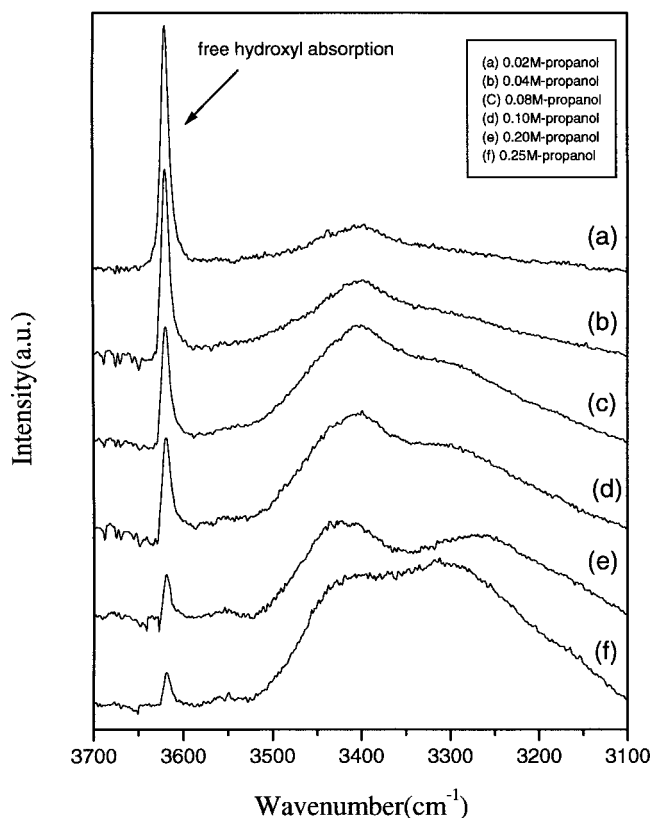


Figure 3. The free hydroxyl band absorption of 4-ethylphenol at the concentration of 0.02 M 4-ethylphenol and concentrations of: (a) 0.02 M; (b) 0.04 M; (c) 0.08 M; (d) 0.10 M; (e) 0.20 M; (f) 0.25 M.

Table 1. The f_m^{OH} and K_A of 4-ethylphenol in cyclohexane solution with various 2-propanol concentrations

Conc. of 2-propanol (mole/l)	Corrected intensity of IR absorption	f_m^{OH}	K_A (mol/L)
0.02	0.096	0.703	30.00
0.04	0.075	0.545	26.98
0.08	0.051	0.372	25.02
0.10	0.048	0.352	21.11
0.20	0.033	0.241	17.02
0.25	0.030	0.215	15.59

decreases with the increase of the 2-propanol content, indicating that the hydrogen bonding exists between these two components. However, the free hydroxyl band of the 2-propanol can also affect the intensity of the free hydroxyl band of Eph and the corrected intensity of absorption in this situation have been widely discussed in our previous study [24]. Table 1 summarizes the fraction of free hydroxyl group of the Eph from various 2-propanol cyclohexane concentrations. The method proposed by Coggesthall and Saier methodology is expressed by the following equation:

$$K_A = \frac{1 - f_m^{\text{OH}}}{f_m^{\text{OH}}(C_A - (1 - f_m^{\text{OH}})C_B)}, \quad (4)$$

where C_A and C_B denote concentrations of 2-propanol and ethylphenol in molL^{-1} , f_m^{OH} represents the fraction

of free hydroxyl of the ethylphenol which is defined as follows:

$$f_m^{\text{OH}} = \frac{I}{I_0}, \quad (5)$$

where $I_0 = a_F^{\text{OH}} \cdot b \cdot c$ and I is intensity of the free hydroxyl band. The a_F^{OH} is the absorptivity coefficient of ethylphenol (34.2) has that obtained previously by Hu et al. [25], b is the path length (0.2 mm) and c is the concentration. The reliable value of 29.58 for K_a is obtained from the approaching zero concentration. However, the conversion of the inter-association equilibrium constant of the 2-propanol into the phenoxy repeat segment is simply given by $29.58 \times 76.56/222.6 = 10.17$ (the molar volume of 2-propanol is $75.56 \text{ cm}^3/\text{mol}$ and the molar volume of phenoxy repeat is $226.6 \text{ cm}^3/\text{mol}$, as calculated from group contribution method) [21]. K_a must be modified into K_A by dividing the molar volume of the PVPh repeated unit (0.1 Lmol^{-1} at 25°C) [21] due to difference molar volume between low molecular weight compound and polymer. The inter-association equilibrium constant, K_A , yielded through this procedure is 101.7. The inter-association constant for the PVPh/phenoxy blend is significantly higher than self-association constants of PVPh and phenoxy, revealing that the tendency to form inter-hydrogen bonding between PVPh and phenoxy is stronger than forming the intra-hydrogen bonding of PVPh and phenoxy in the blend. Therefore, the blend of PVPh/phenoxy is expected to be miscible in the amorphous phase based on the relative magnitude of the inter-association and the self-association constant ($K_A/K_B > 1$). It is understandable that the inter-association equilibrium constant obtained from model compounds is not exactly same as that from the polymer blend due to chain stiffness such as intramolecular screening and functional group accessibility effect in a polymer blend [26–31]. For our knowledge, no suitable equation is available to transform the K_A obtained from model compounds to the K_A of the polymer blend when two polymers possess self-association nature. The hydroxyl stretching in infrared spectra is too complicated to differentiate and determine fractions of non-hydrogen bonding hydroxyl group from both individual homopolymers due to significant overlapping. In this study, we attempt to compare the relative magnitude of inter- and self-association equilibriums based on the classical Coggesthall and Saier methodology.

Thermal Analyses

Differential scanning calorimetry (DSC) has been widely used to investigate the miscibility in polymer blends. Figure 4 shows DSC thermograms of PVPh/phenoxy blends with various compositions, revealing that essentially all PVPh/phenoxy blends give only a single T_g . A single T_g is commonly accepted as evidence of fully miscible in the amorphous phase. Figure 5 shows the dependence of the T_g on the composition of this miscible PVPh/phenoxy blend system where a negative T_g deviation from additive rule on all compositions is observed. In our previous study, we

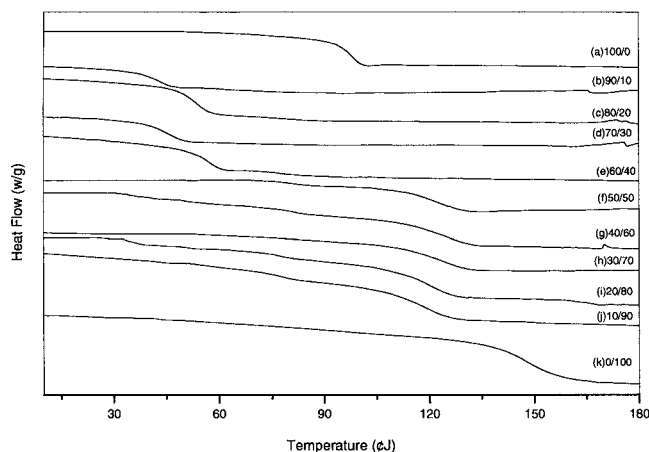


Figure 4. The DSC scans of PVPh/phenoxy blends with different composition: (a) 100/0; (b) 90/10; (c) 80/20; (d) 70/30; (e) 60/40; (f) 50/50; (g) 40/60; (h) 30/70; (i) 20/80; (j) 10/90; (k) 0/100.

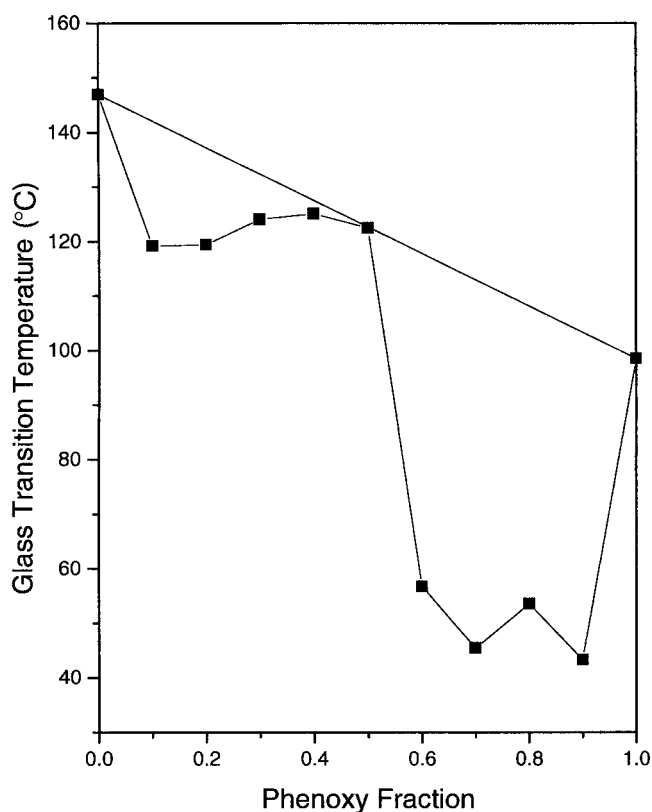


Figure 5. T_g versus composition curves.

have also found that a similar negative deviation in the phenolic/phenoxy blend system [32–34]. The negative T_g deviation can be interpreted as that strong self-association of PVPh and phenoxy was removed and free volume is increased by blending each other. Therefore, the observed negative T_g behavior in this PVPh/phenoxy system indicates that not only the PVPh and phenoxy are miscible, but also a special interaction exists between these two homopolymers. In general, the T_g deviation is a result of entropy change corresponding to the change in the number of hydrogen bonding interaction. In this study, the phenoxy molecule contains a longer repeat unit and thus possesses a relatively smaller number of potential hydrogen bonding sites avail-

able of forming the inter-association hydrogen bonding. The reduction in entropy by forming the inter-association hydrogen bonding between PVPh and phenoxy is not great enough to overcome the entropy increase associated with the breaking off of the self-associations of both PVPh and phenoxy. As a result, the negative maximum T_g deviation is observed of these PVPh/phenoxy blends.

FTIR Analyses

FTIR measurements provide further information concerning the specific interaction existing in polymer blend systems. The hydroxyl stretching in the infrared spectrum is sensitive to the hydrogen bonding formation. Figure 6 shows scale-expanded infrared spectra in the range 2700–4000 cm^{-1} of PVPh and phenoxy recorded at various temperatures. The ratio of free hydroxyl stretching area (A_f) can be using the iterative least-square computer program that has been used to obtain the best fit of the recorded spectrum in this region. A linear baseline was drawn from 4000 to 3100 cm^{-1} to facilitate the curve fitting procedure. It was confirmed that there are three Gaussian peaks in this hydroxyl-stretching region [32]. Figure 6(a) shows that the PVPh has the absorption band at 3540 cm^{-1} that is attributed to the free hydroxyl. Broad bands at 3470 cm^{-1} and 3360 cm^{-1} are assigned as the wide distribution of dimer and multimer hydrogen bonded hydroxyls at 150 °C, respectively. Meanwhile, in Figure 6(b), the peak of the pure phenoxy at 3580 cm^{-1} is contributed by the free hydroxyl while the broad bands observed at 3510 cm^{-1} and 3420 cm^{-1} are attributed to a wide distribution of dimer and multimer hydrogen bonded hydroxyls. The change of the infrared spectra shown in Figure 6 agrees with the expectation of decreasing number of the hydrogen bonded hydroxyl at a higher temperature that has been well-documented. Figure 7 shows scale-expanded infrared spectra in the range 2700–4000 cm^{-1} of various PVPh/phenoxy blends recorded at 150 °C. We choose IR spectra at 150 °C because this temperature is above T_g s of both components and therefore, it is reasonable to assume that an equilibrium condition for specific interaction is obtained. The ratio of the area of the free hydroxyl absorption to the total area of the hydroxyl absorption, A_f , is used here as an index to infer the extent of the free hydroxyl existing in a blend. The frequency ν , the width at half-height $w_{1/2}$, and the A_f of the free hydroxyl band are presented in Table 2 and Figure 8. Figure 8 shows that the trend of A_f matches well with T_g behavior over the entire compositions. The higher A_f value implies less amount of hydrogen bonding between PVPh and phenoxy. PVPh/phenoxy = 90/10 and 30/70 show two maximum A_f and two minimum T_g s. Therefore, these two compositions give the maximum negative T_g deviation that are consistent with the lowest A_f values. Interestingly, the glass transition temperature behavior at PVPh/phenoxy = 50/50 obeys the additive rule. This particular composition has highest fraction of hydrogen bonding that is also consistent with FTIR results. This obtained result confirms that the T_g reduction is due to the increased fraction of the free hydroxyl in PVPh/phenoxy blends.

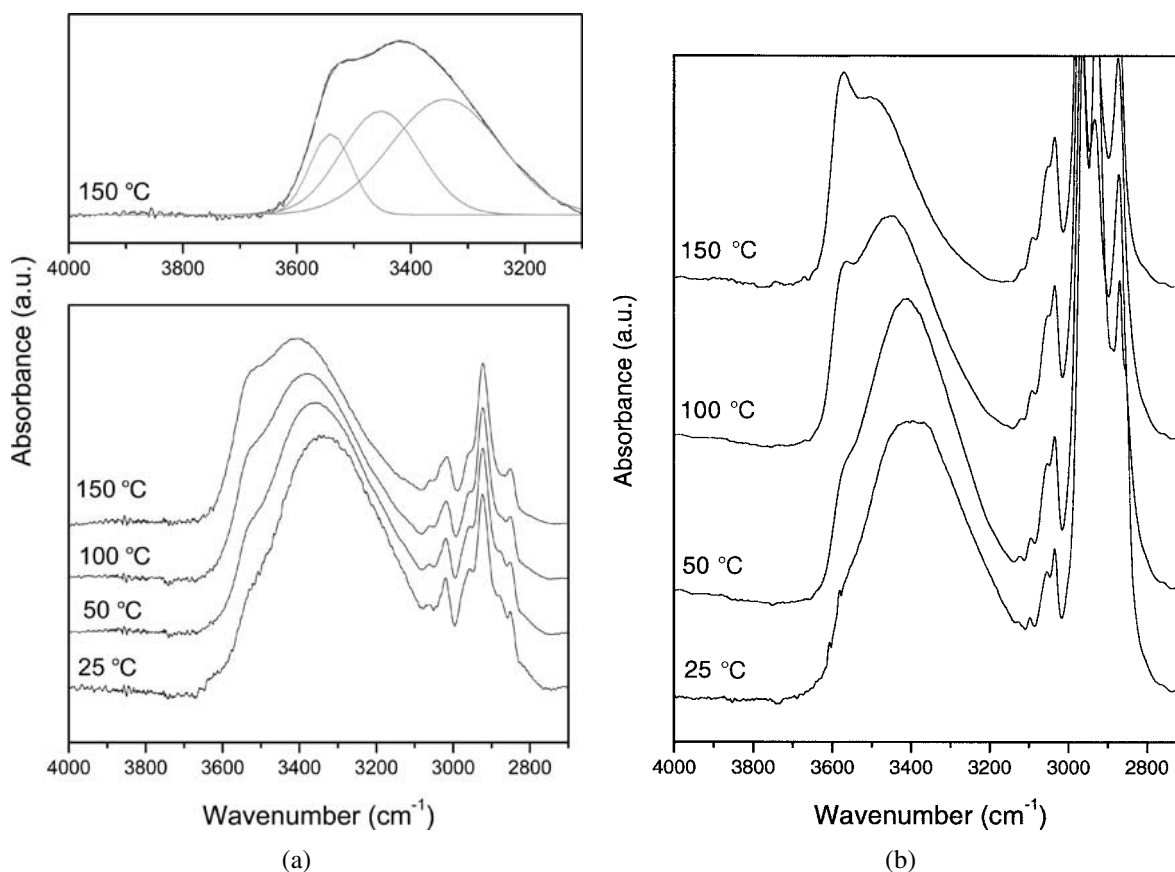


Figure 6. FTIR spectra of the hydroxyl-stretching range of the (a) pure PVPh and (b) pure phenoxy at various temperatures.

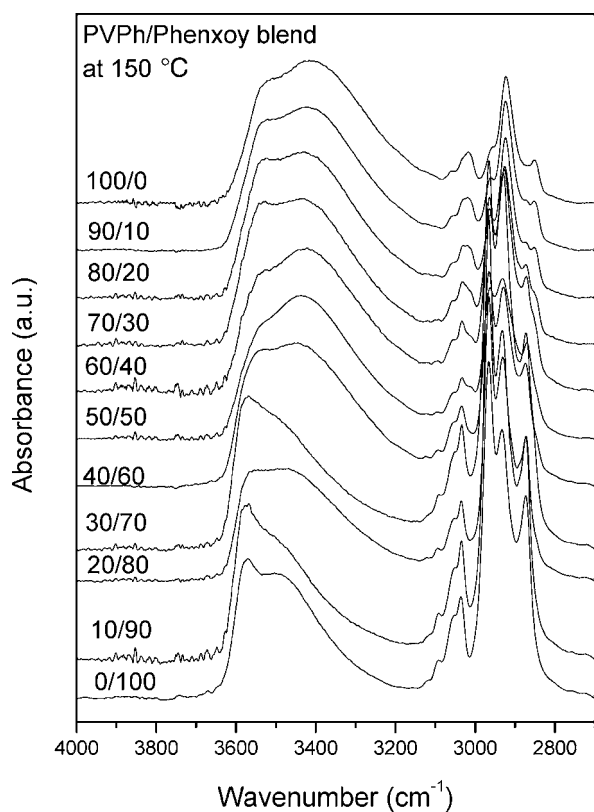


Figure 7. FTIR spectra recorded at 150 °C at 4000 cm^{-1} –2700 cm^{-1} region for PVPh/phenoxy blends: (a) 100/0; (b) 90/10; (c) 80/20; (d) 70/30; (e) 60/40; (f) 50/50; (g) 40/60; (h) 30/70; (i) 20/80; (j) 10/90; (k) 0/100.

Table 2. Curve-fitting from IR spectra at 150 °C of PVPh, phenoxy and their blend

Composition (PVPh/phenoxy)	Free hydroxyl		
	ν (cm^{-1})	$w_{1/2}$ (cm^{-1})	A_f (%)
100/0	3541.7	68.3	10.3
90/10	3544.5	76.3	17.5
80/20	3547.6	72.9	17.1
70/30	3551.9	74.6	15.6
60/40	3555.7	72.0	14.2
50/50	3555.6	71.6	13.8
40/60	3563.8	66.5	16.3
30/70	3580.2	49.7	18.9
20/80	3573.1	53.0	14.2
10/90	3580.2	47.5	16.4
0/100	3578.3	73.2	11.3

ν : wavenumber; $w_{1/2}$: half-height width; A_f : free hydroxyl area ratio.

Solid State NMR Analyses

Solid state NMR spectroscopy can also provide information on the specific interaction of polymer blends involving the hydrogen bonding formation. The ^{13}C CP/MAS spectra of pure PVPh, phenoxy and their blends are shown in Figure 9. The pure PVPh has six major resonance peaks and the hydroxyl-substituted carbon in the phenolic ring (C-6) is at 153.2 ppm. Seven peaks can also be observed from the phenoxy, and the resonance at 69.4 ppm is from the hydroxyl

carbon (C-7). The main peak assignments for PVPh and phenoxy shown in Figure 9 are given in Figure 1. The hydrogen bonding donated carbon produces a small perturbation to the magnetic shield on the nucleus and results in a downfield chemical shift compared with the ones without the hydrogen bonding formation. On the contrary, the electron-accepted carbon tends to shift upfield in the chemical shift. Figure 10 shows the chemical shifts of the hydroxyl-substituted carbon in PVPh (C-6) and in phenoxy (C-7). The C-6 resonance of the PVPh component shifts downfield gradually with

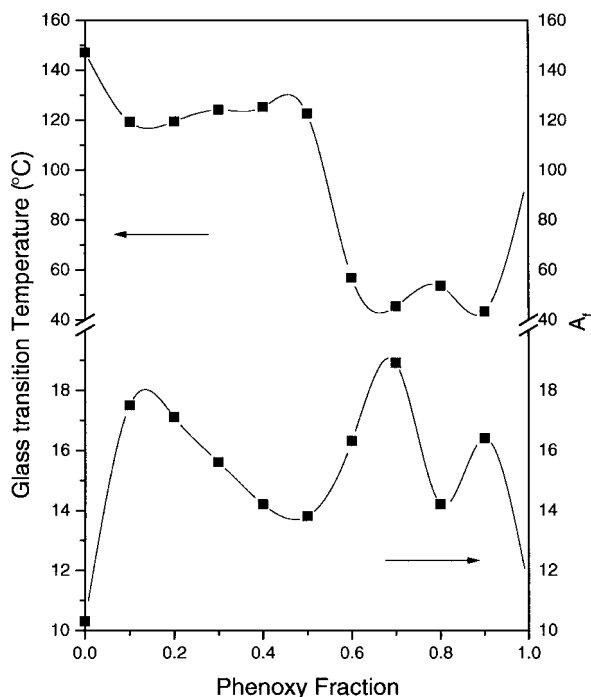


Figure 8. T_g and A_f versus phenoxy content of the PVPh/phenoxy blends.

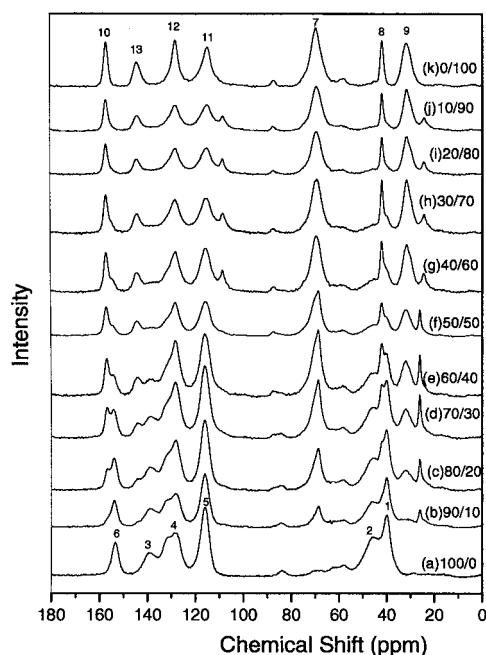


Figure 9. ^{13}C CPMAS spectra at room temperature for PVPh/phenoxy blends: (a) 100/0; (b) 90/10; (c) 80/20; (d) 70/30; (e) 60/40; (f) 50/50; (g) 40/60; (h) 30/70; (i) 20/80; (j) 10/90; (k) 0/100.

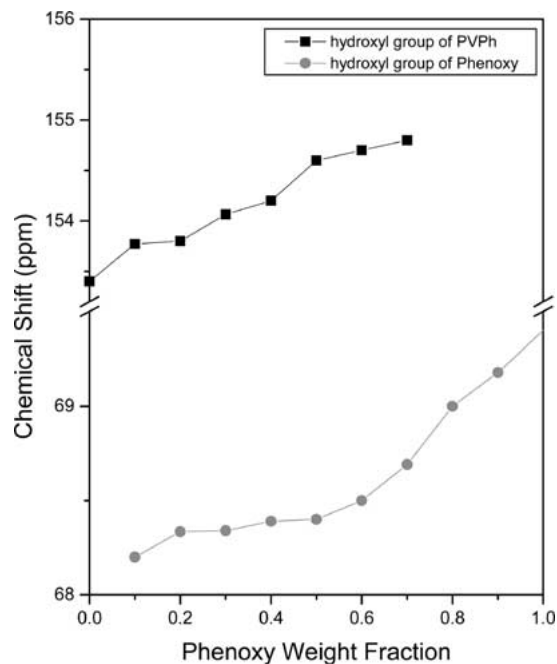


Figure 10. Composition dependence of the chemical shift of hydroxyl group of PVPh (●) and the hydroxyl substituted carbon of phenoxy (■) in the PVPh/phenoxy blends.

increasing phenoxy content. On the contrary, the C-7 resonance of the phenoxy shifts upfield with increasing PVPh content, indicating that the hydroxyl group of the phenoxy tends to be an electron-accepted carbon. Taking into account these two relatively magnitudes of inter- and self-association equilibrium constants of PVPh and phenoxy, the $K_A/K_C = 3.97$ of the phenoxy is greater than the $K_A/K_B = 1.52$ of PVPh, indicating that the inter-hydrogen bonding formation is more favorable for the phenoxy polymer chain. As a result, the hydroxyl-substituted carbon of the phenoxy shifts upfield due to the electron density drawing into the phenoxy polymer chain. This result is also consistent with previous infrared spectra and T_g behavior that the hydrogen bonding exists between these two polymers.

Conclusions

PVPh and phenoxy are completely miscible in the amorphous phase over the entire composition range due to the inter-association hydrogen bonding from the hydroxyl of PVPh and the hydroxyl of phenoxy. FTIR and solid-state NMR studies provide positive evidence of the inter-hydrogen bonding formation between these two self-associating polymers. According to Painter–Coleman association model, the inter-association equilibrium constant for the PVPh/phenoxy blend is significantly higher than self-association equilibrium constants of PVPh and phenoxy, indicating that the hydrogen bonding between PVPh and phenoxy is more favorable than the self-association hydrogen bonding of PVPh or phenoxy.

Acknowledgement

The authors thank the National Science Council, Taiwan for financially supporting this research under Contract NSC-90-2216-E-009-026.

References

1. S. W. Kuo and C. F. Chang, *Macromolecules*, **34**, 5224 (2001).
2. P. Iriondo, J. J. Iruin and M. J. Fernandez-Berride, *Macromolecules*, **29**, 5605 (1996).
3. P. Pedrosa, J. A. Pomposo, E. Calahorra and M. Cortazar, *Macromolecules*, **27**, 102 (1994).
4. S. H. Goh, S. Y. Lee, X. Luo, M. W. Wong and K. L. Tan, *Macromol. Chem. Phys.*, **202**, 31 (2001).
5. E. G. Lezcano, D. R. Arellano, M. G. Prolongo and C. S. Coll, *Polymer*, **39**, 1583 (1998).
6. M. V. Meftahi and J. M. J. Frechet, *Polymer*, **29**, 477 (1988).
7. J. J. Sotele, V. Soldi and A. T. N. Pires, *Polymer*, **38**, 1179 (1997).
8. D. J. T. Hill, A. K. Whittaker and K. W. Wong, *Macromolecules*, **32**, 5285 (1999).
9. H. L. Chen, H. H. Liu and J. S. Lin, *Macromolecules*, **33**, 4856 (2000).
10. J. Wang, M. K. Cheung and Y. Mi, *Polymer*, **42**, 3087 (2001).
11. C. J. Serman, Y. X. Paul, P. C. Painter and M. M. Coleman, *Polymer*, **32**, 516 (1991).
12. C. J. Serman, P. C. Painter and M. M. Coleman, *Polymer*, **32**, 1049 (1991).
13. J. Q. Zhao, E. M. Pearce and T. K. Kwei, *Macromolecules*, **30**, 7119 (1997).
14. M. Alberdi, E. Espi, M. J. Fernandez-Berride and J. J. Iruin, *Polymer Journal*, **26**, 37 (1994).
15. M. M. Coleman and E. J. Moskala, *Polymer*, **24**, 251 (1983).
16. M. Iriarte, E. Espi, A. Etxeberria, M. Valero, M. J. Fernandez-Berride and J. J. Iruin, *Macromolecules*, **24**, 5546 (1991).
17. C. Uriarte, J. I. Eguiazabal, M. Llanos, J. I. Iribarren and J. J. Iruin, *Macromolecules*, **20**, 3038 (1987).
18. Y. Ward and Y. Mi, *Polymer*, **40**, 2465 (1999).
19. A. M. Ilarduay, J. J. Iruin and M. J. Fernandez-Berride, *Macromolecules*, **28**, 3707 (1995).
20. J. Dai, S. H. Goh, S. Y. Lee and K. S. Siow, *Polymer*, **37**, 3259 (1996).
21. M. M. Coleman, J. F. Graf and P. C. Painter, *Specific Interactions and the Miscibility of Polymer Blends*, Technomic Publishing, Lancaster, PA, 1991.
22. E. Espi, M. Alberdi and J. J. Iruin, *Macromolecules*, **26**, 4586 (1993).
23. N. D. Coggesthall and E. L. Saier, *J. Am. Chem. Soc.*, **71**, 5414 (1951).
24. H. D. Wu, P. P. Chu and M. C. C. Ma, *Polymer*, **39**, 703 (1997).
25. Y. Hu, H. R. Motzer, A. M. Etxeberria, M. J. Fernandez-Berride, J. J. Iruin, P. C. Painter and M. M. Coleman, *Macromol. Chem. Phys.*, **201**, 705 (2000).
26. P. C. Painter, B. Veytsman, S. Kumar, S. Shenoy, J. F. Graf, Y. Xu and M. M. Coleman, *Macromolecules*, **30**, 932 (1997).
27. M. M. Coleman, G. J. Pehlert and P. C. Painter, *Macromolecules*, **29**, 6820 (1996).
28. G. J. Pehlert, P. C. Painter, B. Veytsman and M. M. Coleman, *Macromolecules*, **30**, 3671 (1997).
29. G. J. Pehlert, P. C. Painter and M. M. Coleman, *Macromolecules*, **31**, 8423 (1998).
30. M. M. Coleman, K. S. Guigley and P. C. Painter, *Macromol. Chem. Phys.*, **200**, 1167 (1999).
31. P. C. Painter and M. M. Coleman, *Polymer Blends*, Vol. 1, D. R. Paul, Ed., Wiley, New York, 2000.
32. H. D. Wu, C. C. M. Ma and P. P. Chu, *Polymer*, **38**, 5419 (1997).
33. H. D. Wu, P. P. Chu, C. C. M. Ma and F. C. Chang, *Macromolecules*, **32**, 3097 (1999).
34. H. D. Wu, C. C. M. Ma and F. C. Chang, *Macromol. Chem. Phys.*, **201**, 1121 (2000).